Separation Science and Technology
Publication details, including instructions for authors and subscription information:
http://www.informaworld.com/smpp/title~content=t713708471

Complete Decalcification of Saline Effluent by Associating a Carboxylic Resin with a Chelating Resin

C. Fargues[a]; B. Broyart[a]; M. Benmami[b]; M. L. Lameloise[a]
[a] ENSIA-UMR Génie Industriel Alimentaire, Massy cedex, France [b] LIMHP-CNRS, J.B.Clément-Université Paris, Villetaneuse, France

To cite this Article Fargues, C. , Broyart, B. , Benmami, M. and Lameloise, M. L.(2006) 'Complete Decalcification of Saline Effluent by Associating a Carboxylic Resin with a Chelating Resin', Separation Science and Technology, 41: 2, 359 — 377
To link to this Article: DOI: 10.1080/01496390500459452
URL: http://dx.doi.org/10.1080/01496390500459452

Separation Science and Technology, 41: 359–377, 2006

ISSN 0149-6395 print/1520-5754 online
DOI: 10.1080/01496390500459452

Complete Decalcification of Saline Effluent by Associating a Carboxylic Resin with a Chelating Resin

C. Fargues and B. Broyart
ENSIA-UMR Génie Industriel Alimentaire, Massy cedex, France

M. Benmami
LIMHP-CNRS, J.B.Clément-Université Paris, Villetaneuse, France

M. L. Lameloise
ENSIA-UMR Génie Industriel Alimentaire, Massy cedex, France

Abstract: Saline effluent from the glucose industry can be reused as resin regenerants after treatment by a bipolar membrane electrodialysis process preceded by chromatographic decalcification. Ca^{2+}/Na^{+} isotherms measured on two weak acidic resins showed that the chelating resin has a higher selectivity for calcium. The decalcification process was optimized by combining rough decalcification on a carboxylic resin, followed by a finishing step on a chelating one. This chromatographic system led to the expensive chelating resin being spared and to the treatment of 60% more volume of effluent than with the carboxylic resin alone.

Keywords: Decalcification of saline effluent, glucose industry, ion exchange chromatography, carboxylic resin, chelating resin modeling

INTRODUCTION

One of industry's ways of producing glucose is by enzymatic hydrolysis of wheat or corn starch. The syrup produced has to be purified before being

Received 23 August 2005, Accepted 30 October 2005
Address correspondence to C. Fargues, ENSIA-UMR Génie Industriel Alimentaire, 1 av. Des Olympiades, 91744 Massy cedex, France. Tel.: 33 1 69 93 50 93; Fax: 33 1 69 93 50 44; E-mail: fargues@ensia.fr

commercialized; one of these purification steps consists in demineralization on cationic and anionic ion exchange resins, in order to remove the major anions and cations it contains: the cations concerned are mainly Na^+, Ca^{2+}, and K^+. Once the resins are saturated, they need to be regenerated respectively with HCl and NaOH solutions. Resulting effluent contains not only NaCl at high concentration, but also calcium salts. This effluent is then spread or concentrated before crystallization. Bipolar membrane electrodialysis has proved to be a valuable process for its treatment and valorization, as it is able to convert a salt into its acid and base components, in this case HCl and NaOH solutions that could be recycled as resin regenerants during demineralization (1, 2). The use of bipolar membrane electrodialysis is limited by the presence of divalent cations. Because of the production of hydroxyl ions at the anodic side of the membranes, hydroxide precipitates may lead to membrane fouling, inducing a loss of membrane permselectivity and an increase in their electric resistance. The calcium concentration of the feed solution must therefore be previously limited to 1 or 2 ppm; a limit above which the structure of the cationic membranes may be damaged.

In a previous study, A. Gonin (3, 4) has shown that pre-treatment of this effluent could be obtained through conventional electrodialysis (for effluent concentration), followed by ion-exchange chromatography to retain calcium ions. Electrodialysis led to an extremely high proportion of sodium ion (35000 ppm) compared to that of calcium (300 ppm) in the concentrated effluent produced. To complete decalcification, giving a calcium concentration as low as 2 ppm in these conditions, the use of a chelating resin was shown to be necessary (3). Actually, these ion-exchangers are known to develop coordination bonds between metal cations and the chelating groups, leading to high selectivities (5). A study of this step led to the choice of amino-phosphonic groups as chelating sites, being more selective for the alkaline metals than the iminodiacetate chelating groups. A neutral pH was also shown to increase the resin capacity (3, 6). Nevertheless, the use of a chelating resin for such an application is limited by its price; at least twice that of a carboxylic one, and also by the higher consumption in regeneration solutions that arises from its selectivity for divalent species. The study presented here concerns the optimization of the decalcification of concentrated effluent by association of two ion-exchange resins. Due to its selectivity, the chelating resin is still thought to be efficient for very low calcium concentration ranges (and proportions). The idea is therefore to keep this expensive resin in order to finish decalcification, after a first rough decalcification achieved with a cheaper carboxylic resin. This study was carried out on synthetic mixtures containing only calcium and sodium chlorides, with concentrations corresponding to typical industrial effluent. The combination of the two ion-exchange chromatographic steps was explored experimentally as well as numerically. For modelling purposes at the preparative scale, equilibrium ion-exchange data on each of the resins were needed. They were obtained by the dynamic method on columns. Then, the efficiencies of

each of the chromatographic steps—first separately and then combined—were compared.

EXPERIMENTAL: MATERIALS AND PROCEDURE

Ion Exchange Isotherms

The ion exchange and chelating resins were supplied by Rohm and Haas Co (USA). The carboxylic resin used was IMAC HP336 and the chelating resin was Duolite C467 with amino-phosphonic groups as chelating agents. The physical properties of both resins are given in Table 1. They are both weak cationic exchangers:

amino-phosphonic group (chelating Duolite C467 resin)

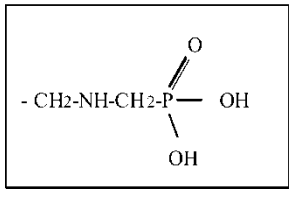

carboxylic group (carboxylic IMAC HP336 resin)

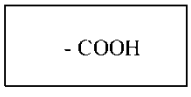

The Ca^{2+}/Na^{+} ion-exchange equilibrium can be written as follows:

$$2(R-Na) + Ca^{2+} \overset{K_{Ca/Na}}{\rightleftharpoons} R_2 - Ca + 2Na^{+} \quad (1)$$

with I and R-I, the ion species in the liquid and solid phases respectively, and $K_{Ca/Na}$ the thermodynamic equilibrium constant.

In the following, the ion exchange equilibrium will be described by the mass action law, using the rational selectivity coefficient K (expressed

Table 1. Physical properties of the resins used

	IMAC HP336	Duolite C467
Matrix	Modified acrylic copolymer	Styrene-DVB copolymer
Functional group	$-COO^{-}$	$-CH_2-NH-CH_2-PO_3^{2-}$
Exchange capacity ($\sim q_{tot}$)	>3.9 eqL^{-1} (H^{+} form)	>1 eqL^{-1} (Na^{+} form)
Average beads diameter	550–750 μm	500–700 μm
Moisture content	54–58 (w% H^{+} form)	65–70 (w% Na^{+} form)

relative to ionic fractions):

$$K = \frac{y_{Ca}}{x_{Ca}} \frac{x_{Na}^2}{y_{Na}^2} \tag{2}$$

or

$$K = \frac{y_{Ca}}{x_{Ca}} \frac{(1 - x_{Ca})^2}{(1 - y_{Ca})^2} \tag{3}$$

with

$x_{Ca} = [Ca]/N =$ calcium ionic fraction in the solution $(-)$

$y_{Ca} = [R_2{-}Ca]/q_{tot} =$ calcium ionic fraction in the solid phase $(-)$

$N =$ solution normality (eqL^{-1})

$q_{tot} =$ total ion exchange capacity (eqg^{-1}).

As the exchange concerns heterovalent species, the coefficient K depends on the solution normality N and on the total exchange capacity q_{tot} of the solid phase. For each resin, all the experimental points of the equilibrium $y_{Ca} = f(x_{Ca})$ ion exchange curve should thus be obtained for the same solution normality N, and with a total ion exchange capacity q_{tot} unchanged. The resins' active sites being weak acid groups, the total capacities of the resins are supposed to change to a certain extent with pH (5, 7). Therefore, the measurement of the isotherms was performed under a controlled and constant pH, adjusted to 7 to optimize the chelating resin performances (3). The ionic strength chosen for the present study corresponds to that of the industrial effluent obtained after concentration by conventional electrodialysis, i.e. $N = 1.54\ \text{eqL}^{-1}$.

Calcium Analysis

Calcium concentrations were measured by atomic absorption spectrophotometry (Varian Techtron Spectrophotometer, AA-1275 series) with an air-acetylene flame. Calibration solutions were made by dilution of a $1\ \text{gL}^{-1}$ calcium standard solution (Labosi–Fisher Scientific, France) with deionized water. They contained the same quantity of sodium chloride as the diluted solutions to be analyzed, in order to take into account molecular absorption due to the high content of this salt.

Measurement of Ion-Exchange Isotherms

For each resin, about $50\ \text{cm}^3$ was put into the sodium form by column conditioning with at least $12BV$ ($BV =$ Bed Volume) of 1 M NaOH followed by rinsing with deionised water until a neutral pH was obtained.

The Ca^{2+}/Na^{+} mixtures were made from pure crystallised NaCl (min 99%) and $CaCl_2$, $2H_2O$ for analysis (min 99.5%) (Labosi–Fisher Scientific, France). They were made so as to correspond to the same solution normality $N = 1.54$ eqL^{-1} and their pH was adjusted to 7 with small amounts of 0.01 M NaOH or HCl solutions. Their calcium concentrations C_{Ca} were measured and the corresponding calcium fractions calculated as $x_{Ca} = C_{ca}/N$. The equilibrium data were obtained by fixed bed experiments at room temperature, by the frontal analysis method. Some batch experiments were also performed to ensure that equilibrium was reached in the column. For each equilibrium point, a glass column of 6.6 mm I.D. and 120 mm long was filled with a sample of the previously conditioned fresh resin, leading to a maximum bed volume of 4.1 cm^3 (Omnifit–Fisher Bioblock Scientific, France). The column was fed until saturation with a solution of given composition x_{Ca}, the effluent collected globally (V_{global}) and its average concentration $C_{Ca\,global}$ measured. Afterwards, the column was emptied, the resin filtered and let to dry at 105°C until constant weight m. The fixed calcium quantity q_{Ca} in equilibrium with C_{Ca} was calculated according to:

$$q_{Ca} = \frac{[(C_{Ca} - C_{Ca\,global}) \cdot V_{global} - C_{Ca} \cdot V_0]}{m} \tag{4}$$

with

q_{Ca} = calcium capacity of the resin at equilibrium with C_{Ca} (eqg^{-1} dry resin)

C_{Ca} = calcium concentration in the influent (eqL^{-1})

$C_{Ca\ global}$ = calcium concentration in the collected effluent (eqL^{-1})

V_{global} = collected effluent volume (L)

V_0 = extra-column and column porosity volume (L)

m = dry resin weight (g)

The y_{Ca} resin composition was obtained by dividing the calcium capacity q_{Ca} obtained by the total ionic exchange capacity of the resin q_{tot}, measured in a similar way but with a pure calcium chloride solution of $C_{Ca} = 1.54$ eqL^{-1} ($x_{Ca} = 1$). Several experiments were carried out, for x_{Ca} between 0 and 1. For each resin, the rational selectivity coefficient K (Eq. (3)) was optimized according to a least square non linear minimization method (Matlab version 6.1).

Breakthrough Curves Study

Residence Time Distribution

The residence time distributions (RTD) were measured for both carboxylic and chelating columns in the sodium form, using stepwise injections of

Blue Dextran as a tracer. The extra-column contributions were taken into account by measuring the RTD on the extra-column system in the same way. The mean residence time (t_s) of the tracer as well as the standard deviation σ inside the columns were then deduced. This led to $\varepsilon = 0.4$ in the case of the Duolite C467 column and $\varepsilon = 0.43$ for the IMAC HP336 one, and to a number of mixing cells $J = 20$ in both cases.

In a column, the Peclet number is given by: $Pe = (u/porosity) \cdot (L)/(D_{ax})$. Considering that for $J > 10$, the Peclet number is related to J by $Pe = 2J$ (8), D_{ax} values could be estimated: $D_{ax} = 4 \times 10^{-6}\,m^2s^{-1}$ in the case of the Duolite C467 column and $D_{ax} = 2.4 \times 10^{-6}\,m^2s^{-1}$ for the IMAC HP336. These data are necessary for the calculation of V_0 in Eq. (4), as well as for the columns modelling.

Calcium Retention on each Resin Separately

Fresh resins initially conditioned in sodium form, as previously described, were used. The glass columns were low pressure Omnifit columns (Fisher Bioblock Scientific, France) and the flow-rates were chosen according to the advice of the resin supplier.

The feed synthetic solution was made similar to the industrial pre-treated effluent:

$$C_{Ca} = 300 \text{ ppm or } 0.015\,eqL^{-1} \qquad C_{Na} = 35000 \text{ ppm or } 1.52\,eqL^{-1}$$

which corresponds to a calcium fraction $x_{Ca} = 0.01$ and $N = 1.54\ eqL^{-1}$.

Samples were collected at the outlet of each column with a Gilson 201/C collector for calcium analyses and measurements of breakthrough curves. At least three breakthrough curves were developed on each column; the resin being regenerated between two successive runs.

The IMAC HP336 resin was loaded in a 10 mm I.D. column. Its bed height was adjusted to 14.4 cm with a piston, giving an initial bed volume in the sodium form of $BV_{IMAC} = 11.3\,cm^3$. The flow-rate was set at $81\,cm^3\,h^{-1}$ (or $7.2\ BV\,h^{-1}$). From the breakthrough curve obtained, a mass balance on the column allowed the calcium capacity to be calculated (to be compared to the isotherm result obtained previously).

The second purpose of this experiment was to obtain the critical feed volumes V_1 and V_2, necessary for the further combination of the carboxylic and the chelating resins. V_1 is the feed volume passed onto the carboxylic IMAC column until the calcium concentration in the effluent reaches the value of 2 ppm ($x = 6.5 \times 10^{-5}$). With this composition, the effluent can be sent directly to the bipolar membrane electrodialysis process without any risk of membrane fouling with calcium hydroxide precipitates. V_2 volume corresponds to an outlet calcium concentration of 100 ppm ($x = 0.0033$). This value was chosen arbitrarily as being the calcium concentration that should not be exceeded in the chelating resin feed, in order to spare this expensive

medium. The chelating column would then receive a feed of calcium composition of between 2 and 100 ppm.

For the Duolite C467 resin, a 15 mm I.D. column was used, and the bed height adjusted to 14.7 cm leading to an initial bed volume in the sodium form of $BV_{Duolite} = 26\,cm^3$. The flow-rate was set at $270\,cm^3h^{-1}$ (or $10.4\ BVh^{-1}$). The breakthrough curve obtained enabled us to calculate the calcium capacity according to a mass balance on the column.

Description of Cyclic Operation

Two 10 mm I.D. columns were used. Resins heights were adjusted to $L = 14.4\,cm$ for the IMAC HP336 column ($BV_{IMAC} = 11.3\,cm^3$) and $L = 10.5\,cm$ for the Duolite C467 one ($BV_{Duolite} = 8.25\,cm^3$). The global resin bed volume was thus $19.55\,cm^3$. The flow-rate was set at $81\,cm^3h^{-1}$, corresponding to $7.2\ BVh^{-1}$ for the IMAC column and $9.8\ BVh^{-1}$ for the Duolite resin. The following process then took place (Fig. 1).

- First, the IMAC was fed with a V_1 volume of synthetic solution. It corresponds to a calcium concentration in the column outlet lower than 2 ppm. The IMAC effluent was collected globally for a further calcium concentration analysis ($C_{global1}$).

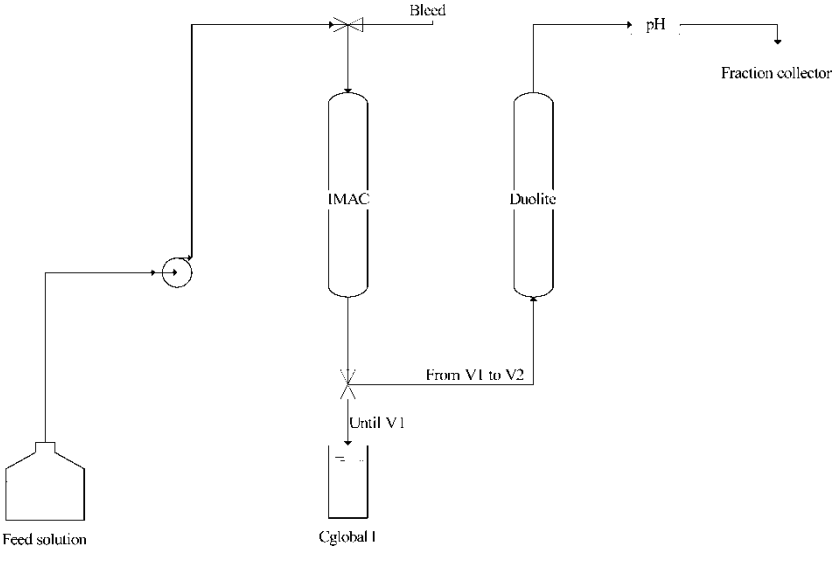

Figure 1. Decalcification cyclic operation unfolding: rough decalcification on carboxylic IMAC HP336 column, followed by complete decalcification on a chelating Duolite C467 column.

- From V_1 to V_2, the IMAC column outlet was connected to the Duolite column entrance. During this step, the chelating resin was supposed to receive a feed calcium composition of between 2 and 100 ppm. Fractions were collected at the Duolite outlet for further analyses. The last collected fraction concentration was called C_{final}.
- When V_2 was reached, the IMAC HP336 column was partially saturated with the synthetic solution. The flow was then stopped and the connection with the chelating column top was closed. The IMAC resin was then regenerated using 7*BV* of 1 M HCl, followed by 6*BV* of 1 M NaOH solution and 5*BV* deionized water rinse. The HCl regeneration effluent was globally collected for further calcium analysis ($C_{global2}$).

A second cycle could then take place. The chelating resin was not regenerated between two cycles.

RESULTS AND DISCUSSION

Ion-Exchange Equilibrium Isotherms

The curvature of the isotherms obtained (Fig. 2) shows that the exchange is extremely favorable to calcium adsorption. We can see a high degree of scatter of the experimental points especially in the range of low calcium fractions, for which the analytical precision is the worst. Both resins differ

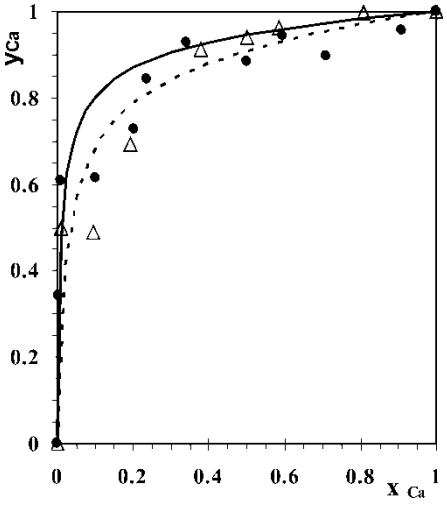

Figure 2. Ca^{2+}/Na^{+} ion-exchange isotherms on IMAC HP336 and Duolite C467 resins. ($T = 20°C$, $N = 1.54$ eqL^{-1}, pH = 7). △, – – –: IMAC HP336, experimental and model ($K = 56$); •, ———: Duolite C467, experimental and model ($K = 166$).

regarding their total capacity q_{tot}, with 7.1 $meqg^{-1}$ (1.78 eqL^{-1} Na^+ form) for the Duolite C467 and 12.6 $meqg^{-1}$ (3.63 eqL^{-1} Na^+ form) for the IMAC HP336 (Table 2). These values are in line with the capacities indicated by the resins supplier (Table 1). Even if it exhibits a lower total capacity, the K parameter for the Duolite resin is three times that of the carboxylic one, leading to a ionic fraction y_{Ca} 60% higher than that of the carboxylic resin for the concentration under study ($x_{Ca} = 0.01$). Consequently, the corresponding calcium capacities expressed in $meqg^{-1}$ are almost identical for both resins; about 3.5 $meqg^{-1}$ (Table 2).

Such isotherm curvature should lead to compressive calcium concentration profiles in both columns (9). But as the calcium fraction of the synthetic effluent under study is below 1% (x_{Ca} about 0.01), only the beginning of the isotherm curves (which seems linear in this concentration region) will have any impact on the shape of adsorption profiles and on the associated breakthrough curves. Considering this, a linear representation for y = f(x) could have met the adsorption behavior well in the case studied here. But yet, if x_{Ca} exceeds 2–3%, as could be the case in industrial effluent, the isotherm becomes strongly non-linear, and such equation would not be viable any more.

Fixed-Bed Studies

In order to predict calcium retention during the cycles using the association of carboxylic and chelating resins, a classical mathematical description of ion exchange in the fixed-beds was used (5, 10, 11). The bed was treated as a continuous medium with assumption of a local equilibrium between liquid and sorbent, and of plug-flow of the stream, taking axial dispersion into account. In the following, x and y notations concern the calcium ionic fractions:

- Mobile phase differential mass balance:

$$\frac{\partial x}{\partial t} + \frac{q_{tot}}{\varepsilon N}\frac{\partial y}{\partial t} + \frac{u}{\varepsilon}\frac{\partial x}{\partial z} = D_{ax}\frac{\partial^2 x}{\partial z^2} \tag{5}$$

Table 2. Ion-exchange capacities and selectivity coefficients

	IMAC HP336	Duolite C467
q_{tot}	12.6 $meqg^{-1}$ 3.63 eqL^{-1} (Na^+ form)	7.1 $meqg^{-1}$ 1.78 eqL^{-1} (Na^+ form)
K	56	166
Calculated values for		
$x_{Ca} = 0.01$: $-y_{Ca}$	0.29	0.47
$-q_{Ca}$	3.65 $meqg^{-1}$	3.34 $meqg^{-1}$

with

u = linear velocity (ms^{-1})

ε = bed porosity (−)

D_{ax} = axial dispersion coefficient (m^2s^{-1})

Taking into account the equilibrium isotherm relation (3) in the $\partial y/\partial t$ expression, equation (5) becomes:

$$\frac{\partial x}{\partial t} = -\frac{u/\varepsilon}{1 + q_{tot}/\varepsilon N(\partial y/\partial x)}\frac{\partial x}{\partial z} + \frac{D_{ax}}{1 + q_{tot}/\varepsilon N(\partial y/\partial x)}\frac{\partial^2 x}{\partial z^2} \tag{6}$$

- Initial and boundary conditions:

$$x = 0, y = 0 \quad \text{at} \quad t = 0 \tag{7}$$

$$\left.\frac{\partial x}{\partial z}\right|_{z=0} = \frac{u}{\varepsilon D_{ax}}(x|_{z=0} - x_{alim}) \quad \text{at} \quad z = 0,\ t > 0 \tag{8}$$

$$\left.\frac{\partial x}{\partial z}\right|_{z=L} = 0 \quad \text{at} \quad z = L,\ t > 0 \tag{9}$$

with L = column length (m).

After a spatial discretization of these equations, the ordinary differential equations system obtained was solved numerically according to a Matlab programme using ODE15s solver (Matlab version 6.1). It allows the calculation of the calcium breakthrough curve ($x = f(t)$ at the outlet of the column $z = L$), as well as the calcium profile inside the column ($x = f(z)$, for $t = t_{final}$).

Decalcification on each Resin Separately

Repeated breakthrough curves were developed until saturation, on each resin separately in the conditions previously described.

On the IMAC HP336 column (Fig. 3), we observe that the calculated stoichiometric breakthrough obtained by simulation 1 occurs sooner and is much steeper than the experimental one. The shape difference could be explained by an underestimation of the axial dispersion coefficient D_{ax}, or by the fact that no transfer kinetics (external film nor intra-particular diffusions) was taken into account in the model. It was decided to improve the simulation only by acting on the axial dispersion coefficient. Further work should be undertaken to improve the model and take transfer kinetics into account. Concerning the capacity, integration of the experimental breakthrough curves leads to an average resin capacity $q_{Ca} = 5.6\,meqg^{-1}$ (for $x_{Ca} = 0.0122$) which corresponds to

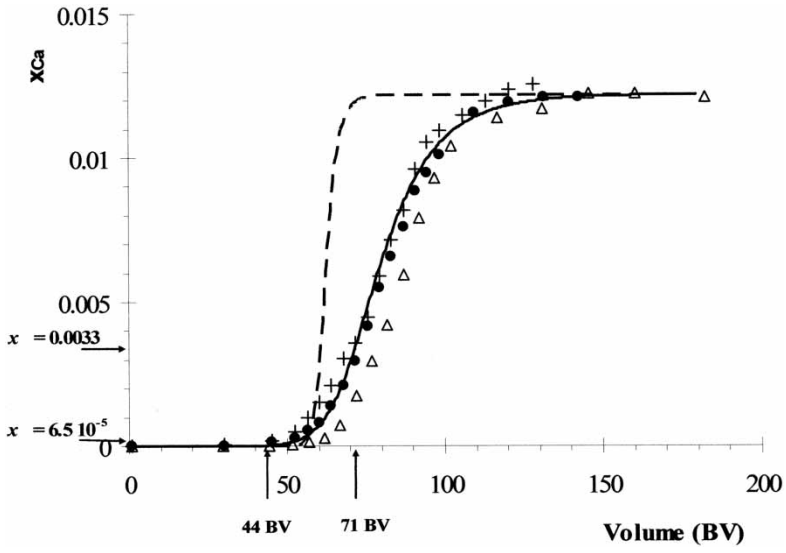

Figure 3. Experimental and calculated calcium breakthrough curves on the carboxylic IMAC HP336 column. Parameters: $BV = 11.3\,cm^3$; $D = 10\,mm$; flow-rate = 81 $cm^3\,h^{-1}$; $x_{Ca\ feed} = 0.0122$; $pH = 7$; $N = 1.54\ eqL^{-1}$; $\Delta z = 6 \times 10^{-4}\,m$; $\Delta t = 250\,s$. +: experiment 1; •: experiment 2; △: experiment 3; – – –: Simulation 1 ($K = 56$, $D_{ax} = 2.4 \times 10^{-6}\,m^2\,s^{-1}$); ———: Simulation 2 ($K = 100$, $D_{ax} = 1.5 \times 10^{-5}\,m^2\,s^{-1}$).

$y_{Ca} = 0.44$, 30% higher than the theoretical $y_{Ca} = 0.33$ obtained with $K = 56$ and Eq. (3). This underestimation is probably due to the fact that K was optimized on the entire range of the experimental (x_{Ca}, y_{Ca}) values, from 0 to 1. Figure 2 shows that the calculated isotherm curve with $K_{opt} = 56$ does not fit the beginning of the isotherm well. The influence of K on the calculated ion-exchange equilibrium for the IMAC HP336 resin is shown on Fig. 4; it demonstrates that $100 < K < 145$ leads to a better estimation of the isotherm region of $x_{Ca} < 1\%$. The simulated breakthrough curve obtained with $K = 100$ and spread according to a $D_{ax} = 1.5 \times 10^{-5}\,m^2\,s^{-1}$ fits the experimental results much better (Fig. 3–Simulation 2). Both parameters will be kept for further simulations.

Concerning the Duolite C467 column: despite the excessive steepness of the simulated breakthrough curve, the optimized selectivity coefficient $K = 166$ gives a good estimation of the experimental breakthrough volume (Fig. 5–Simulation 1). Integration of the breakthrough curves leads to an average experimental capacity $q_{Ca} = 3.84\,meqg^{-1}$ (for $x_{Ca} = 0.015$), corresponding to $y_{Ca} = 0.54$, identical to the theoretical value $y_{Ca} = 0.54$ obtained from Equation (3). As for the IMAC column, an increase of D_{ax} to $5 \times 10^{-5}\,m^2\,s^{-1}$ is necessary to give a better estimation of the experimental spreading (Fig. 5–Simulation 2).

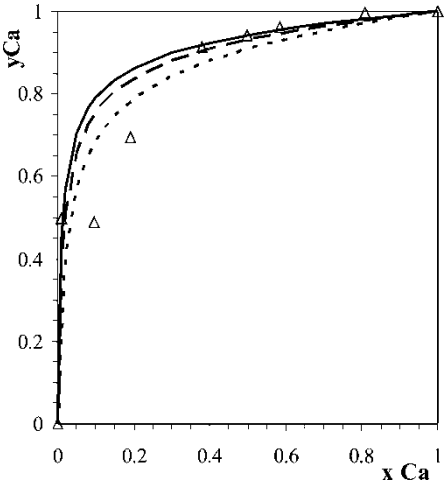

Figure 4. Influence of the rational selectivity coefficient K on the simulated curve for the IMAC HP336 isotherm. △:experiment; ——$K = 145$; – – $K = 100$; . . . . .$K = 56$.

Decalcification Cycles: Combination of the Carboxylic and the Chelating Resins

The experimental IMAC breakthrough curve alone allowed values of V_1 and V_2 volumes for the decalcification cycles to be chosen: calcium concentration

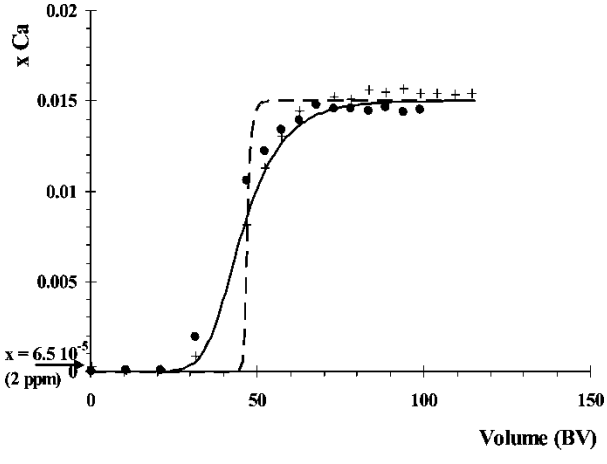

Figure 5. Experimental and calculated calcium breakthrough curves on the chelating Duolite C467 column. Parameters: $BV = 26\,\mathrm{cm}^3$; $D = 15\,\mathrm{mm}$; flow-rate $= 270\,\mathrm{cm}^3\,\mathrm{h}^{-1}$; $x_{Ca\ feed} = 0.015$; $pH = 7$; $N = 1.37\ \mathrm{eqL}^{-1}$; $K = 166$; $\Delta z = 5 \times 10^{-4}$ m; $\Delta t = 250\,\mathrm{s}$. •: experiment 1; +: experiment 2; – – –: Simulation 1 ($D_{ax} = 4 \times 10^{-6}\,\mathrm{m}^2\mathrm{s}^{-1}$); ———: Simulation 2 ($D_{ax} = 5 \times 10^{-5}\,\mathrm{m}^2\,\mathrm{s}^{-1}$).

of the effluent reaches 2 ppm ($x_{Ca} = 6.5 \times 10^{-5}$) for $V_1 \sim 44BV_{IMAC}$, and 100 ppm ($x_{Ca} = 0.0033$) for $V_2 \sim 71BV_{IMAC}$. The experimental breakthrough between these two calcium concentrations is thus spread over $27BV_{IMAC}$ ($\sim 300\,cm^3$).

The most interesting results concerning the decalcification cycles are reported in Table 3. The calcium concentration measured in the IMAC effluent collected from 0 to V_1 ($C_{global1}$) are always lower than 2 ppm, in adequation with the electrodialysis process constraint, as expected. Concerning the second treatment step relative to the Duolite C467 column, it can be seen that after 8 combination cycles, the effluent collected is still below 2 ppm with a calcium composition of the last fraction collected (C_{final}) at the 7th and 8th cycles of about 0.5 ppm (Fig. 9). The experiments were not further pursued (until reaching the critical value of 2 ppm in the column outlet), so we could not check what the maximal effluent volume treated that way would have been. Regeneration of the chelating resin would then have been necessary.

The calcium fixed by the carboxylic IMAC HP336 column during each cycle was quantified globally by the measurement of calcium concentration in the regeneration effluent ($C_{global2}$) and calculation of $Q = C_{global2} \times$ Regenerant Volume (Table 3). This quantity, adsorbed during the IMAC feed with $71BV_{IMAC}$ of initial solution, is about 13 meq whatever the cycle. This shows that from the beginning, the IMAC column behaves identically throughout the successive feed and regeneration runs. The integration of the IMAC breakthrough curve of Fig. 3 until $71BV_{IMAC}$ leads to an average adsorbed quantity of 14 meq. We conclude that the experimental breakthrough obtained on the IMAC HP336 column alone (Fig. 3) well represents the calcium retention on the IMAC column during the cycles.

The comparison of decalcification results for each resin separately and their combination shows that for similar bed volumes (i.e. $BV = 19.55\,cm^3$), the column combination leads to a higher treated volume. Indeed, the critical calcium value of 2 ppm had not been reached at the end of the 8th combination cycle, showing that by that process, more than $8 \times 800\,cm^3 = 6.4\,L$ of effluent can be treated with regeneration of only the carboxylic resin column. On a similar bed volume of chelating resin alone (i.e. $BV_{Duolite} = 19.55\,cm^3$), the critical 2 ppm value would be reached for $508\,cm^3$ ($=26BV_{Duolite}$, Fig. 5) after which the resin needs to be regenerated. Eight

Table 3. Decalcification cycles results

Cycles	1	2	3	4	5	6	7	8
$C_{global1}$ (mgL^{-1})	0.47	0	0	0	1	0.82	0.82	0.3
Q (meq)	13	12.7	13.1	14.1	13.2	12.3	13.5	—
C_{final} (mgL^{-1})	0.08	0	0	0	0.3	0.3	0.6	0.4

feed/regeneration cycles would have therefore produced only 4 L of decalcified solution. In fact, if the chelating resin is used alone, it receives an influent calcium composition of $x_{Ca} \sim 0.01$ instead of $6.5 \times 10^{-5} < x_{Ca} < 0.0033$ through the combination, and is then more rapidly saturated. Considering that the global cost of resin would have been higher than in the combination situation and that the regeneration efficiency of the chelating resin would have been probably less than that of the carboxylic one, the use of the chelating resin alone for this application is not economically viable.

Compared to the decalcification result obtained with the carboxylic column alone, the combination of resins means that 60% effluent volume more per cycle can be treated (800 cm^3 decalcified, compared to 500 cm^3 for $BV_{IMAC} = 11.3\ cm^3$ in both cases). This is obtained for the same regenerant consumption, given that during eight cycles, the chelating bed did not need to be regenerated.

The high decalcification performance reached by the combination process may be explained by the high selectivity of the chelating resin for Ca^{2+}, with $K = 166$. Indeed, for calcium composition as low as $6.5 \times 10^{-5} < x_{Ca} < 0.0033$, this resin still exhibits a good capacity, with y_{Ca} lying between 0.0106 and 0.283: the chelating resin is still efficient for the retention of calcium traces.

Modelling of the Calcium Retention Cycles

We simulated the calcium retention by the chelating resin, fed by the outlet of the IMAC column during the cycles. The carboxylic IMAC column breakthrough curve was first calculated and its calcium composition for the volumes lying between $44BV_{IMAC}$ and $71BV_{IMAC}$ used as repeated numerical feed for the Duolite column (Fig. 6). Except for the first cycle for which the chelating resin was considered as fresh, the internal profile of the chelating column obtained at the end of each previous cycle was used as its initial calcium composition for the following cycle. The simulated breakthrough curve and successive profiles are given on Figs. 7 and 8 respectively.

According to simulation 1 (Fig. 7), corresponding to the equilibrium and axial dispersion coefficients previously adjusted, the 2 ppm limit on calcium concentration should have occurred at the end of the second cycle. For the 8th cycle, the calcium fraction should have reached $x_{Ca} = 5 \times 10^{-4}$ corresponding to 15 ppm, much higher than the value $C_{final} \approx 0.5$ ppm experimentally obtained. A decrease of the axial dispersion coefficient inside the Duolite column ($D_{ax} = 4 \times 10^{-6}\ m^2\ s^{-1}$, as first calculated) leads to a steeper but still premature simulated calcium breakthrough curve (Fig. 7–Simulation 2).

This failure in the prediction of the chelating column experimental breakthrough may be due to an under estimation of the carboxylic IMAC HP336 column capacity for the calcium. As can be seen in Fig. 3, the rational selectivity coefficient $K = 100$ does not fit the third experiment well.

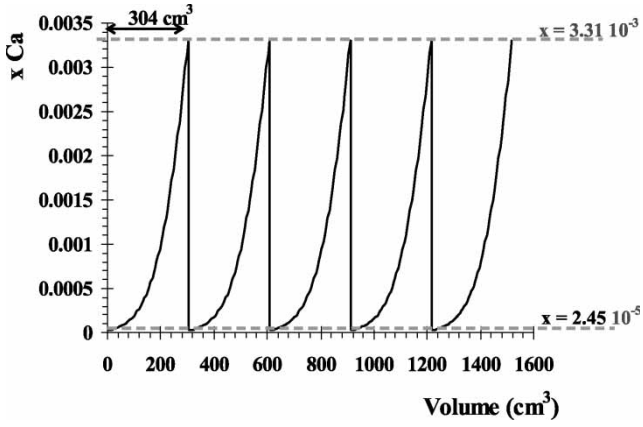

Figure 6. Duolite C467 column feed composition calculated from the simulated IMAC HP336 column breakthrough, between $44BV_{IMAC}$ and $71BV_{IMAC}$. Parameters: $BV = 11.3\,\mathrm{cm}^3$; $D = 10\,\mathrm{mm}$; flow-rate $= 81\,\mathrm{cm}^3\,\mathrm{h}^{-1}$; $pH = 7$; $N = 1.54$ eqL^{-1}; $x_{Ca\ feed} = 0.0114$; $K = 100$; $x_{Ca\ feed} = 0.0114$; $D_{ax} = 1.5 \times 10^{-5}\,\mathrm{m}^2\,\mathrm{s}^{-1}$; $\Delta z = 6 \times 10^{-4}\,\mathrm{m}$; $\Delta t = 250\,\mathrm{s}$.

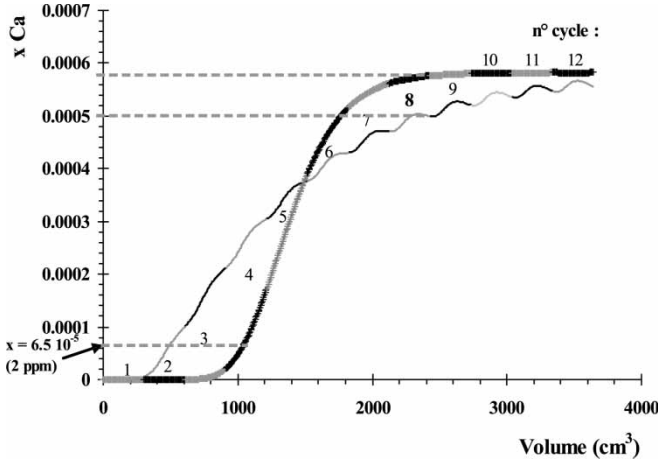

Figure 7. Influence of the axial dispersion coefficient inside the Duolite C467 column on its simulated calcium breakthrough during 12 coupling cycles. Parameters: IMAC: $BV = 11.3\,\mathrm{cm}^3$, $D = 10\,\mathrm{mm}$; flow-rate $= 81\,\mathrm{cm}^3\,\mathrm{h}^{-1}$; $pH = 7$; $N = 1.54$ eqL^{-1}; $x_{Ca\ IMAC\ feed} = 0.0114$; $K = 100$; $D_{ax} = 1.5 \times 10^{-5}\,\mathrm{m}^2\mathrm{s}^{-1}$; $\Delta z = 6 \times 10^{-4}\,\mathrm{m}$; $\Delta t = 250\,\mathrm{s}$. Duolite: $BV = 8.25\,\mathrm{cm}^3$; $D = 10\,\mathrm{mm}$; flow-rate $= 81\,\mathrm{cm}^3\,\mathrm{h}^{-1}$; $pH = 7$; $N = 1.54$ eqL^{-1}; $K = 166$; $x_{Ca\ \ Duolite\ \ feed} =$ IMAC outlet from $44BV_{IMAC}$ to $71BV_{IMAC}$; $\Delta z = 5 \times 10^{-4}\,\mathrm{m}$; $\Delta t = 250\,\mathrm{s}$. ——, Simulation 1 ($D_{ax} = 5 \times 10^{-5}\,\mathrm{m}^2\mathrm{s}^{-1}$), ———, Simulation 2 ($D_{ax} = 4 \times 10^{-6}\,\mathrm{m}^2\,\mathrm{s}^{-1}$).

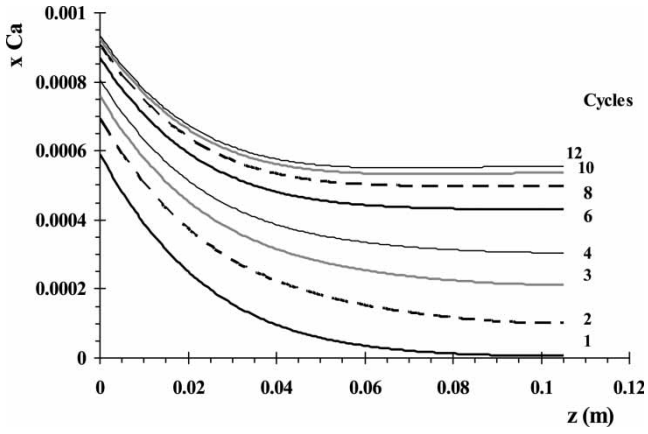

Figure 8. Successive simulated calcium profiles inside the Duolite C467 column during the coupling cycles. Parameters: IMAC: $BV = 11.3\,cm^3$; $D = 10\,mm$; flow-rate $= 81\,cm^3\,h^{-1}$; $pH = 7$; $N = 1.54$ eqL^{-1}; $x_{Ca\ IMAC\ feed} = 0.0114$; $K = 100$; $D_{ax} = 1.5 \times 10^{-5}\,m^2s^{-1}$; $\Delta z = 6 \times 10^{-4}\,m$; $\Delta t = 250\,s$. Duolite: $BV = 8.25\,cm^3$; $D = 10\,mm$; flow-rate $= 81\,cm^3\,h^{-1}$; $pH = 7$; $N = 1.54$ eqL^{-1}; $x_{Ca\ Duolite\ feed} =$ IMAC outlet from $44BV_{IMAC}$ to $71BV_{IMAC}$; $K = 166$; $D_{ax} = 5 \times 10^{-5}\,m^2s^{-1}$; $\Delta z = 5.10^{-4}\,m$; $\Delta t = 250\,s$.

For this breakthrough, a $K = 122$ value would have been more appropriate. Fig. 9 shows the sensitivity of the decalcification simulation with K parameter. A value of at least $K = 145$ better fits the experimental result, with a calcium fraction obtained at the end of the 8th cycle of 1.1 ppm. This K value is not entirely surprising. Indeed, it was shown (Fig. 4) that the scattering of the experimental points was especially high for the small x_{Ca} fractions, and that for $K = 145$, the beginning of the isotherm curve was represented well. Simulation of the combined chromatographic process can thus also be used to refine equilibrium data, which are sometimes difficult to obtain precisely at very low concentrations.

CONCLUSION

The aim of this work was to reach a high degree of decalcification of the glucose industry effluent, concentrated in sodium chloride. This operation is necessary for the further treatment of effluent by bipolar membrane electrodialysis. Ion exchange isotherms Ca^{2+}/Na^{+} were measured on two weak cationic resins and showed a higher selectivity for calcium using chelating resin. The rational selectivity coefficient K was calculated for each support.

The chelating resin being more expensive than the carboxylic one, we developed a chromatographic process in order to optimize the decalcification of this salty effluent and spare the chelating medium. The effluent first passed

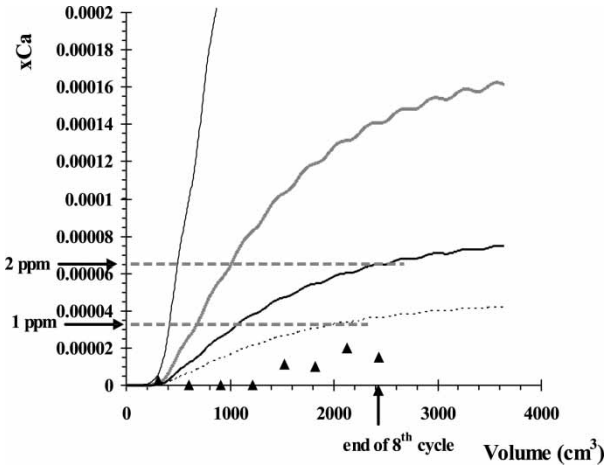

Figure 9. Influence of the rational selectivity coefficient K of the IMAC HP336 resin, on the simulated calcium breakthrough at the outlet of the Duolite C467 resin throughout the combination cycles. Parameters: IMAC: $BV = 11.3\,cm^3$, $D = 10\,mm$; flow-rate $= 81\,cm^3\,h^{-1}$; $pH = 7$; $N = 1.54$ eqL^{-1}; $x_{Ca\ IMAC\ feed} = 0.0114$; $D_{ax} = 1.5 \times 10^{-5}\,m^2s^{-1}$; $\Delta z = 6 \times 10^{-4}\,m$; $\Delta t = 250\,s$. Duolite: $BV = 8.25\,cm^3$; $D = 10\,mm$; flow-rate $= 81\,cm^3\,h^{-1}$; $pH = 7$; $N = 1.54$ eqL^{-1}; $K = 166$; $x_{Ca\ Duolite\ feed} =$ IMAC outlet from $44BV_{IMAC}$ to $71BV_{IMAC}$; $\Delta z = 5 \times 10^{-4}\,m$; $\Delta t = 250\,s$; $D_{ax} = 5 \times 10^{-5}$ m^2s^{-1}. —— $K = 100$; —— $K = 122$; —— $K = 135$; ····· $K = 145$; ▲ experimental points (C_{final}).

through a carboxylic resin was sent to the chelating resin as soon as its calcium concentration reached the critical value of 2 ppm.

In this way, up to 8 cycles of feed and carboxylic column regeneration were conducted without reaching the value of 2 ppm in the chelating column effluent. This combination process enabled 60% more effluent to be treated than did the carboxylic resin alone. Under these conditions, the expensive chelating resin was spared, and used to adsorb calcium ions at very small concentration ranges ($x_{Ca} < 0.4\%$), for which it still exhibits comparatively high retention capacities ($y_{Ca} \rightarrow 28\%$). This also leads to an economy of regeneration solutions, as it is expected that the chelating resin having high affinity for calcium is more difficult to regenerate than the carboxylic one.

Numerical simulations were made for each column alone and for the combined use of resins. They showed that the calcium capacity of the carboxylic resin for the low fractions of interest here had probably been underestimated by the isotherm measurements. An adjustment of the K coefficient on the IMAC HP336 carboxylic resin, which represents the capacity of this resin for calcium, leads to a accurate prediction of the resulting experimental Duolite C467 chelating resin breakthrough.

NOMENCLATURE

BV	Bed volume
C_{Ca}	Calcium concentration in the influent (eqL^{-1})
C_{final}	Calcium concentration of the last fraction collected at the outlet of the Duolite column (eqL^{-1})
C_{global}	Calcium concentration in the collected effluent during isotherm measurements (eqL^{-1})
$C_{global1}$	Calcium concentration of the IMAC column effluent, globally collected from 0 to V_1 (eqL^{-1})
$C_{global2}$	Calcium concentration of the IMAC column regeneration effluent (eqL^{-1})
D_{ax}	Axial dispersion coefficient ($m^2 s^{-1}$)
J	Number of mixing cells in the column
K	rational selectivity coefficient (relative to ionic fractions)
L	Column length (m)
m	Dry resin weight (g)
N	Solution normality (eqL^{-1})
Pe	Peclet number
q_{Ca}	Calcium capacity of the resin in equilibrium with C_{Ca} (eqg^{-1})
q_{tot}	Total exchange capacity of the resin bed (eqg^{-1})
t	Time (s)
t_s	Mean residence time (s)
u	Linear velocity (ms^{-1})
V_0	Extra-column and column porosity volume during isotherm measurements (L)
V_{global}	Collected effluent volume during isotherm measurements (L)
x_{Ca}	Calcium ionic fraction in the solution
y_{Ca}	Calcium ionic fraction in the solid phase
z	Axial position in the column (m)
ε	Bed porosity
σ	Standard deviation inside the column
[ ]	Ionic concentration (eqL^{-1})

ACKNOWLEDGMENT

We are grateful to Rohm and Haas Co (USA) for the free supply of all the resins used in this study.

REFERENCES

1. Bolton, H. (1992) Use of bipolar membranes for ion exchange resin regenerant. *J. Chem. Technol. Biotechnol.*, 54 (4): 341.

2. Bazinet, L., Lamarche, F., and Ipperspiel, D. (1998) Bipolar-membrane electrodialysis: Application of electrodialysis in the food industry. *Trends Food Sci. Technol.*, 9: 107.
3. Gonin, A. (2000) Mise au point d'un procédé de recyclage d'effluents par couplage électrodialyse-échange d'ions. Application aux éluats issus de la régénération de résines de déminéralisation de jus sucrés. Ph.D. Thesis, Université de Montpellier.
4. Gonin, A., Lutin, F., Lameloise, M.L., et al. (1999) Bipolar membranes electrodialysis for recylcling ion exchange resin effluents. In *Récents progrés en Génie des procédés—ECCE2*; Montpellier: Tec & Doc, Lavoisier, Paris, 13 (68), 299.
5. Helfferich, F. (1962) *Ion exchange*; Mc Graw-Hill: New York, N.Y.
6. Meyers, P.S. (1998) How chelating resins behave. *Plat. Surf. Finish*, 85 (10): 22.
7. Vaaramaa, K. and Lehto, J. (1997) H^+/Na^+ exchange in an aminophosphonate-chelating resin. *React. Funct. Polym.*, 33 (1): 19.
8. Villermaux, J. (1993) *Génie de la Réaction Chimique, Conception et Fonctionnement des réacteurs*, 2nd Ed.; Tec & Doc: Lavoisier, Paris.
9. De Vault, D. (1943) The theory of chromatography. *J. Am. Chem. Soc.*, 65: 532.
10. Tondeur, D. and Bailly, M. (1986) Design methods for ion-exchange processes based on the "equilibrium theory". In *Ion Exchange Science and Technology–NATO ASI Series E107*. Rodrigues, A.E. (ed.), Nijhoff, 147.
11. Rodrigues, A.E., Dias, M.M., and Lopes, J.C.B. (1991) Theory of linear and nonlinear chromatography. In *Chromatographic and Membrane Processes in Biotechnology–NATO ASI Series E204*. Costa, C.A. and Cabral, J.S. (eds.), Kluwer Academic Publishers, 25.